

Received: February 19, 2025; Accepted: May 17, 2025; Published: May 18, 2025.

DOI: [10.30473/coam.2025.73788.1292](https://doi.org/10.30473/coam.2025.73788.1292)

Winter-Spring (2025) Vol. 10, No. 1, (33-55)

Research Article



Open Access

Control and Optimization in Applied Mathematics - COAM

Mathematical Modelling of Malaria Spread in Response to Climate Variability in Sudan

Gassan A.M.O. Farah , Abdulaziz Mukhtar , Kailash C. Patidar 

Department of Mathematics and Applied Mathematics, University of the Western Cape, Private Bag X17, Bellville 7535, South Africa.

✉ Correspondence:

Gassan A.M.O. Farah

E-mail:

gfarah@uwc.ac.za

How to Cite

Farah, G., Mukhtar, A., Patidar, K.C. (2025). "Mathematical modelling of malaria spread in response to climate variability in Sudan", *Control and Optimization in Applied Mathematics*, 10(1): 33-55, doi: [10.30473/coam.2025.73788.1292](https://doi.org/10.30473/coam.2025.73788.1292).

Abstract. Malaria continues to represent a significant public health concern in Sudan, with cases rising over 40% from 2015 to 2020. This research investigates how climate change affects malaria transmission patterns using a mathematical model in an ordinary differential equation framework. The analysis involves calculating the basic reproduction number and evaluating the system's qualitative properties to gain insights into disease dynamics. Additionally, a sensitivity analysis is conducted to evaluate how climatic conditions, e.g., rainfall and temperature, influence key model parameters. Statistical approaches are utilized to estimate parameters and calibrate the model using empirical data from Sudan, ensuring consistency between the model and observed trends. Numerical simulations demonstrate the growing influence of climate variability on the spatial distribution of malaria vectors and the transmission progression over time. The study establishes a strong association between climatic changes and the exacerbation of malaria prevalence in Sudan. These findings emphasize the urgent need for climate-adaptive strategies, including improved vector control, strengthened surveillance systems, and climate-resilient public health interventions, to address the increased risks posed by changing environmental conditions. The research provides valuable insights to inform evidence-based policies aimed at reducing malaria transmission in Sudan and other regions that are experiencing similar challenges due to climate change.

Keywords. Malaria, Climate change, Mathematical modelling, Stability analysis, Numerical simulation.

MSC. 92-10; 92B05; 37N25.

<https://matheo.journals.pnu.ac.ir>

©2025 by the authors. Licensee PNU, Tehran, Iran. This article is an open access article distributed under the terms and conditions of the Creative Commons Attribution 4.0 International (CC BY4.0) (<http://creativecommons.org/licenses/by/4.0>)

1 Introduction

Malaria is a lethal disease caused by single-celled parasites, which are primarily transmitted through the bites of infected female *Anopheles* mosquitoes. The lifecycle of these parasites is intricately linked to human hosts, highlighting that humans play a critical role in the disease's transmission dynamics [9, 10]. Recent global data indicates an increase in malaria incidence, with cases per 1,000 population at risk climbing from 57 in 2019 to 82 in 2020 [30]. Notably, Sub-Saharan Africa bears the heaviest toll of malaria, with Sudan emerging as a large contributor to the ongoing malaria crisis in the region [2, 11]. Research indicates that malaria remains a substantial public health issue in Sudan, marked by concerning morbidity and mortality rates [3, 26], particularly among at-risk populations, such as children under five years of age and pregnant women. These groups are disproportionately affected, especially during the rainy season, which exacerbates the transmission of the disease [13].

Climate change is a critical factor influencing mosquito behavior and breeding patterns, thereby increasing the likelihood of malaria outbreaks in endemic regions [17, 21]. Numerous studies highlight how fluctuating climate conditions affect mosquito lifespan and the sporogonic stages of malaria parasites [12, 27]. Elevated temperatures have been correlated with increased mosquito activity, while enhanced rainfall leads to greater populations of mosquito larvae [6]. The importance of average temperatures under varying environmental conditions is crucial for assessing malaria risk in specific geographical areas, as these temperatures profoundly impact the disease's transmission dynamics [8]. Despite notable advancements in malaria control efforts, the challenges presented by climate change threaten to undermine these achievements. This scenario underscores the urgent need for increased awareness, sustained research efforts, and the formulation of effective strategies to mitigate the impact of climate change on malaria transmission [5].

The authors in [18] focused on malaria dynamics in Burundi whereas our focus is on empirical data from Sudan, offering specific insights. Although both studies use deterministic models to assess impact of climate conditions, we develop the model from [25] and incorporated model calibration, sensitivity analysis, as well as empirical validation. Additionally, by rigorous analysis and computational simulations, we investigated the impact of variations in temperature and rainfall on malaria transmission in Sudan.

The potential implications of climate change on malaria distribution are of particular concern. Rising global temperatures may accelerate the spread of malaria to higher altitudes and latitudes, given the sensitivity of both *Anopheles* mosquitoes and *Plasmodium* parasites to temperature variations. These vectors thrive in warm, humid conditions, and climate alterations can enhance their reproductive and feeding activities, potentially reshaping local transmission patterns [22]. Consequently, malaria may re-emerge in areas previously deemed malaria-free, posing significant challenges for public health initiatives.

In countries like Sudan, the effectiveness of malaria control measures is severely hampered by limited resources and socio-economic instability. This research is driven by the persistent challenges posed by malaria in Sudan, despite various control and elimination initiatives. The geographical distribution of malaria is very diverse often influenced by extreme weather events, rainfall patterns, and humanitarian crises arising from ongoing conflicts. Therefore, an integrative approach is essential for effective malaria management, guided by a novel, data-driven climate model. Such a model could yield more

accurate predictions of future malaria incidents, ultimately informing the development of more effective public health policies and interventions.

Mathematical modelling has played a pivotal role in comprehending the dynamics of malaria and identifying optimal control and prevention strategies. These models reveal the direct influence of climate factors, like temperature and rainfall, on vector borne disease (see [1, 6]). Morrise and Hoshen [17] developed a dynamic malaria model incorporating weather-dependent processes in vectors and non-weather-dependent processes in hosts. The authors in [21] devised a simulation model utilizing rule-based modelling to explore climate change's impact on global malaria transmission. Birley [20] formulated a mathematical model to explore the effects of species variation and to assess whether temperature influences the transmissibility of the malaria pathogen *Plasmodium vivax* by the *Anopheles maculipennis* mosquito.

Research conducted by [28, 29] indicates that mosquitoes are most active around dawn and dusk, and prolonged sunlight exposure can dehydrate these insects. Although much remains to be learned about the persistence of diseases transmitted by mosquitoes and malaria transmission in colder seasons, it is generally observed that mosquito activity decreases when temperatures fall below 10°C. During winter, vertebrate hosts serve as the main reservoir for mosquito-borne infections, as the virus remains inactive in colder climates until warmer temperatures allow for reproduction. Female mosquitoes lay eggs that enter a dormant state, freezing or becoming inactive when temperatures drop below 10°C. When the weather warms up, these dormant eggs thaw and initiate mosquito breeding, posing significant health risks to humans. In [29], the authors suggest that ambient temperatures and precipitation levels significantly impact mosquito populations, prompting further investigation into how these factors affect mosquito-borne diseases. Yang [31] proposed a model for malaria transmission that incorporates human acquired immunity levels alongside temperature-dependent parameters of mosquito vectors.

There is an increasing interest in studying the impact of climate change on various vector-borne diseases. The complex relationship between climate variables and malaria transmission requires careful attention to implement effective interventions for a malaria-free future. Although significant progress has been made in malaria modelling, no comprehensive study currently examines the relationship between spatial variations in malaria transmission and climate change in Sudan. Therefore, this study aims to introduce an innovative data-driven dynamic model for malaria transmission that incorporates several key advancements: (i) the use of advanced mathematical techniques combined with climate data to accurately represent the complex dynamics of malaria transmission, and (ii) the integration of data assimilation methods through statistical mean to improve model validation and predictive accuracy.

The rest of the paper is organized as follows. We introduce the deterministic mathematical model, discussing fundamental properties such as positivity, existence of solution, and the derivation of the basic reproduction number in Section 2. We also discuss model calibration process using data of Sudan's weekly malaria cases. We conduct a sensitivity analysis of \mathcal{R}_0 , to identify key parameters influencing disease transmission In Section 3. In Section 4, we explore the global stability of the disease-free equilibrium. We present in Section 5 numerical simulations of the model, which we obtain by using MATLAB solver *ode45*, to illustrate the system's behavior under varying conditions. Finally, in Section 6, we present a summary of our key findings and scope for further research.

2 Mathematical Model Formulation

In this section, we present a deterministic model to illustrate the dynamics of malaria transmission and various control strategies to help combat the disease. This model utilizes compartments associated with “transmission rates” that describe the movement of individuals. By analyzing the transition rates and the size of each compartment over time, it is possible to estimate the overall prevalence and incidence of the disease. This model elucidates the complex interactions between human and mosquito populations, highlighting the critical factors that govern disease transmission and recovery conditions can affect the dynamics of mosquito life cycles but not the host-parasite dynamics.

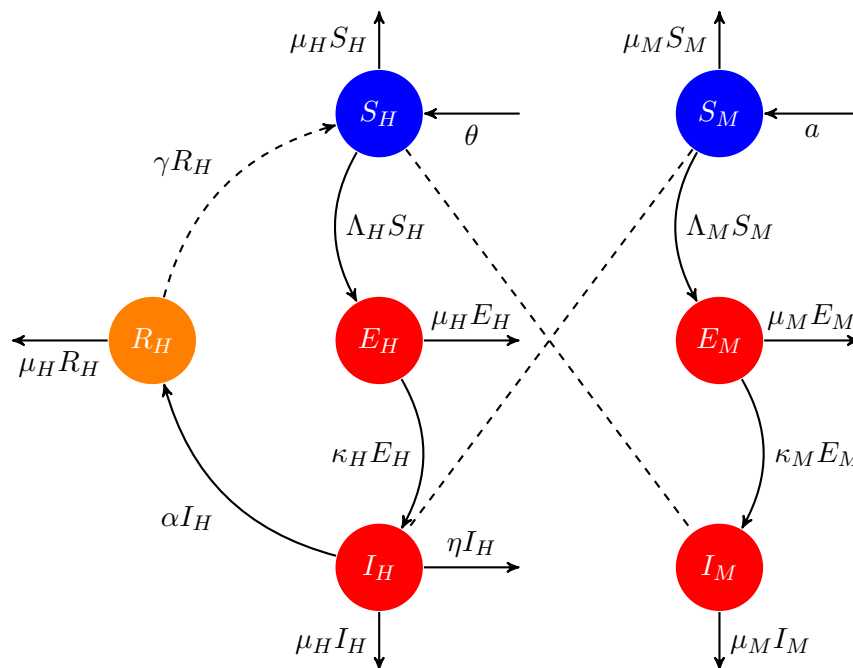


Figure 1: Flow diagram for the *SEIR – SEI* modeling.

The human population, denoted as N_H , is subdivided into four distinct classes: susceptible individuals (S_H), exposed or incubating individuals (E_H), infectious individuals (I_H), and those who have recovered and possess partial immunity (R_H). The prevalence of infection among susceptible individuals is determined by the biting rate ($\epsilon(T, R)$) of mosquitoes, which is influenced environmental conditions, which in this case are, temperature (T) and rainfall (R). Additionally, the proportion of bites from infected mosquitoes that successfully lead to infection (b_H) plays a crucial role. Individuals enter the susceptible population at a constant recruitment rate, denoted by θ , which accounts for both births and immigration. Upon infection, individuals do not immediately transition to the infectious class due to the absence of gametocytes. Instead, they enter the exposed class (E_H), during which the parasite infiltrates the bloodstream in the form of merozoites. Individuals progress from this exposed state to the infectious class (I_H) at a rate of κ_H , where they gain the ability to transmit the disease to susceptible

mosquitoes. The dynamics of infectious diseases in humans are characterized by a gradual build-up of cases followed by rapid escalation and severity. Within the infectious class, individuals recover at a rate represented by α , subsequently moving to the recovered class (R_H) during treatment. It should be noted that not all individuals undergoing treatment will develop temporary immunity. Those who do obtain temporary immunity may lose it over time at a rate of γ and revert to the susceptible class. In contrast, individuals who do not receive treatment for the infection face potential mortality at a rate of η . All compartments of the model are subject to natural mortality, characterized by the rate μ_H . Furthermore, while weather conditions significantly influence mosquito life cycles, they do not impact the intrinsic dynamics of host-parasite interactions.

Now, the population of mosquitoes, denoted as N_M , is also divided into three distinct classes: susceptible (S_M), exposed (E_M), and infectious (I_M). A susceptible mosquito can become infected through a process governed by its biting rate and the probability of transmission per bite represented as b_M . The maturation of aquatic mosquito larvae into adult forms occurs at a rate parameterized as η , influenced by environmental factors such as temperature, rainfall, and the mosquito population's intrinsic mortality rate μ_M . Mosquitoes transition into the exposed class E_M when they acquire gametocytes from blood meals despite the absence of sporozoites in their salivary glands at this stage. A mosquito progresses to the infectious class I_M once it becomes infectious and harbors sporozoites in its salivary glands. These sporozoites have the potential to infect any susceptible host following fertilization. It is important to note that infected mosquitoes experience mortality at a rate μ_M , but they do not clear their infections or exhibit any detrimental health effects. The proposed model comprehensively incorporates various ecological factors that facilitate the transmission of disease, as well as the influence of climatic variables. Critical parameters such as $\epsilon(T, R)$, a , and μ_M are dependent on temperature and rainfall, and are detailed in [16]. These parameters can be quantitatively expressed in equations (1)- (3), elucidating their relationships with climate and impacts on the overall dynamics of mosquito-borne disease transmission, as illustrated in Figures 3 and 4.

$$\epsilon(T, R) = \epsilon_0 \left[\frac{0.48 \exp(0.14(T - 23))}{\exp(-0.14(T - 23)) + \exp(0.14(T - 23))} + \frac{-0.48 \exp(0.32(T - 37))}{\exp(-0.32(T - 37)) + \exp(0.32(T - 37))} \right] \cdot \frac{R}{R + \beta}. \quad (1)$$

$$a(T, R) = \frac{3.375 (4R(50 - R))^3 \exp(-0.00554T + 0.06737)}{50^6 (2 + (0.00554T - 0.06737)^{-1})}. \quad (2)$$

$$\mu_M(T, R) = 0.0886 \exp \left(\left(\frac{-0.01R + 1.01T - 21.211}{14.852} \right)^2 \right). \quad (3)$$

The malaria transmission can be described by the following non-autonomous system

$$\left. \begin{aligned}
 \frac{dS_H}{dt} &= \theta + \gamma R_H - \Lambda_H(T, R)S_H - \mu_H S_H, \\
 \frac{dE_H}{dt} &= \Lambda_H(T, R)S_H - (\kappa_H + \mu_H)E_H, \\
 \frac{dI_H}{dt} &= \kappa_H E_H - (\mu_H + \alpha + \eta)I_H, \\
 \frac{dR_H}{dt} &= \alpha I_H - (\gamma + \mu_H)R_H, \\
 \frac{dS_M}{dt} &= a(T, R) - \Lambda_M(T, R)S_M - \mu_M(T, R)S_M, \\
 \frac{dE_M}{dt} &= \Lambda_M(T, R)S_M - (\kappa_M + \mu_M(T, R))E_M, \\
 \frac{dI_M}{dt} &= \kappa_M E_M - \mu_M(T, R)I_M,
 \end{aligned} \right\} \quad (4)$$

with the initial conditions: $S_H(0) > 0$, $S_M(0) > 0$, $E_H(0) \geq 0$, $E_M(0) \geq 0$, $I_H(0) \geq 0$, $I_M(0) \geq 0$, and $R_H(0) \geq 0$.

Table 1: Model parameters and their corresponding descriptions

Parameters	Description
θ	human recruitment rate
α	human recovery rate
η	death rate due to disease per capita
γ	rate of immunity loss per capita
b_H	likelihood of a susceptible person getting infected from an infected bite
b_M	likelihood of a susceptible mosquito getting infected from an infected person
μ_H	human natural death rate per capita
$\mu_M(T, R)$	mosquito mortality rates dependent on climatic conditions
$a(T, R)$	rate at which aquatic mosquitoes mature into adults
κ_H	rate of progression for the exposed individuals
κ_M	rate of progression for exposed mosquitoes
$\epsilon(T, R)$	mosquito biting rate.

The force of infection rates for humans (Λ_H) and mosquitoes (Λ_M), are defined, respectively, as $\Lambda_H = \frac{\epsilon(T, R)b_H I_M}{N_H}$ and $\Lambda_M = \frac{\epsilon(T, R)b_M I_H}{N_H}$, where

$$N_H = S_H + E_H + I_H + R_H,$$

and

$$N_M = S_M + E_M + I_M.$$

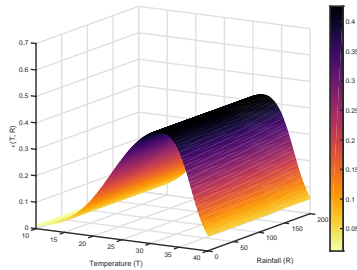


Figure 2: Mosquitoes biting rates as function of (T) and (R) .

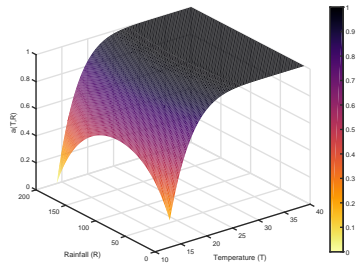


Figure 3: Evolution of mosquito cycles as function of (T) and (R) .

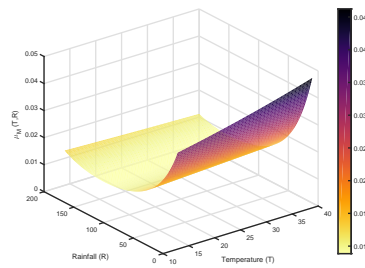


Figure 4: Evolution of mosquito cycles as function of (T) and (R) .

2.1 Positivity of Solutions

Since the model monitors changes in the human population at all times, it is imperative to show all state variables are positive. The analysis of the system (4) should be based on a feasible area of biological

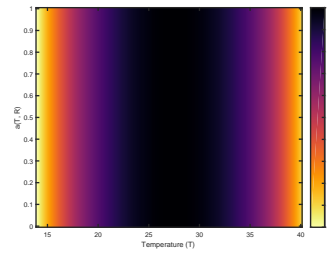


Figure 5: Normalized mosquito biting rate. The color gradient indicates variations in bite rate, with warmer colors showing higher rates and cooler colors showing lower rates.

interest

$$\mathcal{B}_f = \left\{ (S_H, E_H, I_H, R_H, S_M, E_M, I_M) \in \mathbb{R}^7 : S_H + E_H + I_H + R_H \leq N_H, \right. \\ \left. S_M + E_M + I_M \leq N_M \right\}.$$

When the system (4) has non-negative initial data, the solution remains within the set Γ for all time $t > 0$. This means that the set \mathcal{B}_f is positively invariant. The following theorem can be derived from this result.

Theorem 1. Consider the system defined in (4), assuming that the initial conditions for all t satisfy:

$$S_H(0) > 0, E_H(0) \geq 0, I_H(0) \geq 0, R_H(0) \geq 0, S_M(0) > 0, E_M(0) \geq 0, I_M(0) \geq 0,$$

then:

- (1) The solution vector $(S_H(t), E_H(t), I_H(t), R_H(t), S_M(t), E_M(t), I_M(t))$ remains positive for all $t > 0$.
- (2) $\lim_{t \rightarrow \infty} N_H(t) = \frac{\theta}{\mu_H}$,
- (3) if $N_H(0) \leq \frac{\theta}{\mu_H}$, then $N_H(t) \leq \frac{\theta}{\mu_H}$,

Consequently, the region \mathcal{B}_f is positively invariant.

Proof. We will demonstrate this by contradiction. Define X as a bounded set

$$X = \{T \geq 0 \mid S_H(t) > 0, E_H(t) > 0, I_H(t) > 0, R_H(t) > 0 \quad 0 \leq t \leq T\}. \quad (5)$$

Let us denote the supremum of X as T . Given that the initial state variables for all $T > 0$,

$$S_H(0) > 0, E_H(0) > 0, I_H(0) > 0, R_H(0) > 0, S_M(0) > 0, E_M(0) > 0, \text{ and } I_M(0) > 0,$$

we follow the first equation in (4):

$$\frac{dS_H}{dt} = \theta + \gamma R_H - \Lambda_H S_H - \mu_H S_H. \quad (6)$$

Now, consider the function

$$B(t) = \exp \left[\mu_H t + \int_0^t \Lambda_H(s) ds \right], \quad (7)$$

where $B(0) = 1$. Consequently, we have

$$\begin{aligned} \frac{d}{dt} [S_H(t) \cdot B(t)] &= \dot{S}_H(t) \cdot B(t) + S_H(t) \cdot B(t) (\mu_H + \Lambda_H(t)), \\ &= [\theta + \gamma R_H(t)] B(t). \end{aligned} \quad (8)$$

This yields

$$S_H(T) \cdot B(T) - S_H(0) \cdot B(0) = \int_0^T [\theta + \gamma R_H(t)] B(t) dt. \quad (9)$$

Thus, we can rewrite $S_H(T)$ as

$$S_H(T) = B(T)^{-1} \left[S_H(0) + \int_0^T [\theta + \gamma R_H(t)] B(t) dt \right]. \quad (10)$$

Since $B(T) > 0$, $R_H(t) > 0$, and $S_H(0) \geq 0$, we conclude that $S_H(T) > 0$.

By utilizing a similar approach, it can be established that $E_H(t)$, $I_H(t)$, $R_H(t)$, $S_M(t)$, $E_M(t)$ and $I_M(t)$ will also remain positive for $t > 0$. This finding contradicts the premise that T is the supremum of X . Similarly, we conclude that the solutions $S_H(t)$, $E_H(t)$, $I_H(t)$, $R_H(t)$, $S_M(t)$, $E_M(t)$, and $I_M(t)$ from the system described in (4) with non-negative initial conditions will continue to remain non-negative for all times $T > 0$.

Since $N_H = S_H + E_H + I_H + R_H$, the equations in (4) can be summed, yielding:

$$\frac{dN_H}{dt} = \theta - \mu_H N_H.$$

Then, a standard principle [7], the following results are obtained:

$$N_H(t) = \frac{\theta}{\mu_H} + \left[N_H(0) - \frac{\theta}{\mu_H} \right] e^{-\mu_H t}.$$

Therefore,

$$\limsup_{t \rightarrow \infty} N_H(t) = \frac{\theta}{\mu_H},$$

In this context, $N(0)$ denotes the initial value of $N(t)$. It can be noted that if $N(0) \leq \frac{\theta}{\mu}$, then $N(t)$ will also satisfy $N(t) \leq \frac{\theta}{\mu}$ as t approaches infinity. This indicates that $\frac{\theta}{\mu}$ acts as an upper limit for $N(t)$ and, by extension, for all solutions of the system. Conversely, if $N(0) > \frac{\theta}{\mu}$, then $N(t)$ will gradually decrease to $\frac{\theta}{\mu}$ as time progresses toward infinity, indicating that all solutions of the system ultimately converge to $\frac{\theta}{\mu}$. In both scenarios, $\frac{\theta}{\mu}$ remains the upper bound for all solutions. From these findings, it is clear that any solution beginning in the region \mathcal{B}_f will stay within that region indefinitely. Additionally, solutions that start near \mathcal{B}_f will either enter the region immediately or approach it asymptotically over time. Consequently, \mathcal{B}_f is characterized as positively invariant and biologically significant in relation to the flow dictated by the system (4). This ensure the invariance of X . \square

2.2 The Basic Reproduction Number

To assess the model (4) stability, we analyze it as an autonomous system. We start by identifying both trivial and nontrivial equilibrium points in the reduced system. The trivial point, referred to as the disease-free equilibrium (DFE) and denoted by E_0 (see more details in [4]), is obtained by setting all infectious classes to zero in the system (4).

$$E_0 = \left(\frac{\theta}{\mu_H}, 0, 0, 0; \frac{a}{\mu_M}, 0, 0 \right).$$

The readers may note that the basic reproduction number, denoted as \mathcal{R}_0 , represents the average count of new infections generated when a contagious individual enters a population that is entirely susceptible to the disease [15]. Following the notation and approach used in [23], we will use a specific method to calculate the basic reproduction number \mathcal{R}_0 for the system (4). Consequently, the system (4) can be rewritten as follows: Here's a clearer and properly formatted version of your equations:

$$\begin{cases} A_d = f(A_d, A_s), \\ A_s = g(A_d, A_s), \end{cases} \quad (11)$$

where $A_d = (E_H, I_H, R_H, E_M, I_M)^T$ are the infectious compartments and $A_s = (S_H, S_M)^T$ are the disease free. Thus, the DFE of system (4) will be

$$\begin{aligned} A_0^* &= (A_d^*, A_s^*) \\ &= (E_H, I_H, R_H, E_M, I_M, S_H, S_M) \\ &= (0, 0, 0, 0, 0, \theta/\mu_H, a/\mu_H). \end{aligned} \quad (12)$$

According to [15, 19], determining the basic reproduction number requires only involves the compartments of infected individuals. Therefore, utilizing $\frac{dA_d}{dt}$, the system can be expressed as

$$A_d = \mathcal{F}(A) - \mathcal{V}(A),$$

where

$$\mathcal{F}(A) = \begin{bmatrix} \frac{\epsilon b_H I_M S_H}{S_H + E_H + I_H + R_H} \\ 0 \\ 0 \\ \frac{\epsilon b_M I_H S_M}{S_H + E_H + I_H + R_H} \\ 0 \end{bmatrix}, \quad \mathcal{V}(A) = \begin{bmatrix} (\kappa_H + \mu_H) E_H \\ -\kappa_H E_H + (\mu_H + \alpha + \eta) I_H \\ -\alpha I_H + (\gamma + \mu_H) R_H \\ (\kappa_M + \mu_M) E_M \\ -\kappa_M E_M + \mu_M I_M \end{bmatrix}. \quad (13)$$

At DFE A_0^* , the Jacobian matrices \mathbf{F} and \mathbf{V} are as follows:

$$\mathbf{F} = \left[\frac{\partial \mathcal{F}_i}{\partial A_j} \Big|_{A_0^*} \right] = \begin{bmatrix} 0 & 0 & 0 & 0 & \epsilon b_H \\ 0 & 0 & 0 & 0 & 0 \\ 0 & 0 & 0 & 0 & 0 \\ 0 & \Gamma_1 & 0 & 0 & 0 \\ 0 & 0 & 0 & 0 & 0 \end{bmatrix}, \quad \text{and} \quad (14)$$

$$\mathbf{V} = \left[\frac{\partial \mathcal{V}_i}{\partial A_j} \Big|_{A_0^*} \right] = \begin{bmatrix} (\kappa_H + \mu_H) & 0 & 0 & 0 & 0 \\ -\kappa_H & (\mu_H + \alpha + \eta) & 0 & 0 & 0 \\ 0 & -\alpha & (\gamma + \mu_H) & 0 & 0 \\ 0 & 0 & 0 & (\kappa_M + \mu_M) & 0 \\ 0 & 0 & 0 & -\kappa_M & \mu_M \end{bmatrix}. \quad (15)$$

Hence,

$$\mathbf{V}^{-1} = \begin{bmatrix} \Gamma_3 & 0 & 0 & 0 & 0 \\ \Gamma_4 & \Gamma_5 & 0 & 0 & 0 \\ \Gamma_2 & \Gamma_6 & \Gamma_7 & 0 & 0 \\ 0 & 0 & 0 & \frac{1}{\kappa_M + \mu_M} & 0 \\ 0 & 0 & 0 & \frac{\kappa_M}{\mu_M(\kappa_M + \mu_M)} & \frac{1}{\mu_M} \end{bmatrix}, \quad \text{and} \quad (16)$$

$$\mathbf{FV}^{-1} = \begin{bmatrix} 0 & 0 & 0 & \Gamma_8 & \Gamma_9 \\ 0 & 0 & 0 & 0 & 0 \\ 0 & 0 & 0 & 0 & 0 \\ \Gamma_{10} & \Gamma_{11} & 0 & 0 & 0 \\ 0 & 0 & 0 & 0 & 0 \end{bmatrix}, \quad (17)$$

where

$$\begin{aligned} \Gamma_1 &= \frac{ab_H}{\mu_M}, & \Gamma_2 &= \frac{\alpha\kappa_H\kappa_M + \alpha\kappa_H\mu_M^2}{\mu_M(\kappa_M + \mu_M)(\kappa_H + \mu_H)(\mu_H + \alpha + \eta)(\gamma + \mu_H)}, \\ \Gamma_3 &= \frac{1}{\kappa_H + \mu_H}, & \Gamma_4 &= -\frac{-\gamma\kappa_H - \kappa_H\mu_H}{(\kappa_H + \mu_H)(\mu_H + \alpha + \eta)(\gamma + \mu_H)}, \\ \Gamma_5 &= \frac{1}{\mu_H + \alpha + \eta}, & \Gamma_6 &= -\frac{-\alpha\kappa_H - \alpha\mu_H}{(\gamma + \mu_H)(\mu_H + \alpha + \eta)(\kappa_H + \mu_H)}, \\ \Gamma_7 &= \frac{1}{\gamma + \mu_H}, & \Gamma_8 &= \frac{ab_H\kappa_M}{\mu_M(\kappa_M + \mu_M)}, \\ \Gamma_9 &= \frac{\epsilon b_H}{\mu_M}, & \Gamma_{10} &= -\frac{ab_H(-\gamma\kappa_H - \kappa_H\mu_H)}{\mu_M(\gamma + \mu_H)(\mu_H + \kappa_H)(\mu_H + \alpha + \eta)}, \\ \Gamma_{11} &= \Gamma_1\Gamma_5. \end{aligned}$$

The basic reproduction number, \mathcal{R}_0 , is defined as the spectral radius of the next-generation matrix:

$$\begin{aligned} \mathcal{R}_0 &= \rho(\mathbf{FV}^{-1}) \\ &= \sqrt{\frac{\epsilon^2 b_H b_M \kappa_H \kappa_M a}{\mu_M(\mu_H + \kappa_H)(\kappa_M + \mu_M)(\mu_H + \alpha + \eta)}}. \end{aligned} \quad (18)$$

Lemma 1. The disease-free equilibrium point, denoted as E_0 , for the system represented by (4) demonstrates local stability when $\mathcal{R}_0 < 1$ and exhibits instability when $\mathcal{R}_0 > 1$.

2.3 Model Fitting

We used the SEIR-SEI model, as described in the system (4), to calibrate malaria cases in Sudan and project the transmission of the infection over time, with a primary focus on Al-Jazeera state. Our analysis

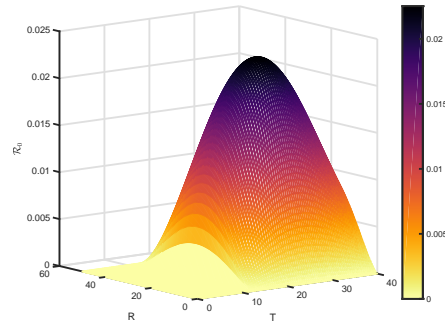


Figure 6: Basic reproduction number (\mathcal{R}_0) as a function of temperature (T) and rainfall (R). The colormap highlights variations in \mathcal{R}_0 under different environmental conditions.

utilized empirical data obtained from the National Malaria Control Program (NMCP) surveillance coordinator at the Federal Ministry of Health (FMOH) in Sudan. This dataset encompasses weekly records of infected individuals over five years, from 2018 to 2022 [24]. We recognize that the data collection process may have inherent limitations, including potential reporting delays, underreporting of cases, and inconsistencies stemming from variable access to healthcare and differences in record-keeping practices across regions. Additionally, external factors such as environmental conditions and socio-economic influences may introduce biases that are challenging to quantify. To mitigate these issues, we validated the data by modeling daily malaria case counts as a Poisson process with a reporting rate denoted by γ . Given the incomplete collection rate, we assumed this reporting rate γ did not exceed 45%. With Poisson observations and constant population size, we utilized the fitR package to fit our model using a ‘fitmodel’ object, which stores relevant variables and functions. We successfully calibrated the model to the initial dataset employing the maximum likelihood estimation method, as illustrated in Figure 7.

Table 2: Parameters values and references

Parameters	Values	Sources
μ_H	0.0000066	fitted data
μ_M	0.00006166	fitted data
ϵ	0.57	fitted data
b_H	0.01	fitted data
b_M	0.02	fitted data
θ	0.0089	fitted data
γ	0.127	fitted data
α	0.250	fitted data
κ_H	0.35	fitted data
κ_M	0.6	fitted data
η	0.00320	fitted data

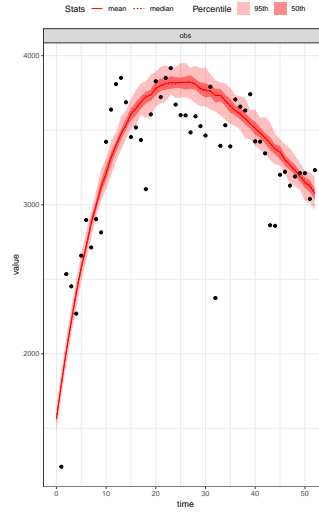


Figure 7: Fitting of Model (4), showing a comparison between the model assessment (represented by the red line) and the data from Sudan (shown as a black dotted line). The parameter estimates obtained from the fitting process are detailed in Table 2.

3 Sensitivity Analysis of \mathcal{R}_0

Sensitivity analysis serves as an essential tool for identifying parameters that significantly influence the dynamics of a system and, consequently, the potential effectiveness of various interventions. In the preceding section, we examined the sensitivity of three parameters to temperature and rainfall. In this section, we expand on this by conducting a sensitivity analysis to evaluate the impact of these key parameters, along with others, on critical model outcomes, specifically focusing on their effect on \mathcal{R}_0 . To assess the model's sensitivity, we compute the partial derivatives of the output variables with respect to the input parameters, normalizing the results. For a given parameter m , the normalized sensitivity index is defined as follows:

$$\Phi_{\mathcal{R}_0}^m = \frac{\partial \mathcal{R}_0}{\partial m} \cdot \frac{m}{\mathcal{R}_0}. \quad (19)$$

The parameters impacting \mathcal{R}_0 in equation (18) in relation to climate include ϵ , and μ_M and a , while α , b_H , b_M , κ_H , κ_M , and η are identified as a parameter that does not exhibit sensitivity to climatic factors. The sensitivity indices for each of these parameters, calculated using formula (19) and illustrated in Figure 8, are as follows:

$$\Phi_{\mathcal{R}_0}^\epsilon = \frac{\partial \mathcal{R}_0}{\partial \epsilon} \cdot \frac{\epsilon}{\mathcal{R}_0}, \quad \Phi_{\mathcal{R}_0}^{\mu_H} = \frac{\partial \mathcal{R}_0}{\partial \mu_H} \cdot \frac{\mu_H}{\mathcal{R}_0}, \quad \Phi_{\mathcal{R}_0}^{\mu_M} = \frac{\partial \mathcal{R}_0}{\partial \mu_M} \cdot \frac{\mu_M}{\mathcal{R}_0}, \quad \Phi_{\mathcal{R}_0}^a = \frac{\partial \mathcal{R}_0}{\partial a} \cdot \frac{a}{\mathcal{R}_0}.$$

Following, those without climate effect are

$$\begin{aligned} \Phi_{\mathcal{R}_0}^{b_H} &= \frac{\partial \mathcal{R}_0}{\partial b_H} \cdot \frac{b_H}{\mathcal{R}_0}, & \Phi_{\mathcal{R}_0}^{b_M} &= \frac{\partial \mathcal{R}_0}{\partial b_M} \cdot \frac{b_M}{\mathcal{R}_0}, & \Phi_{\mathcal{R}_0}^{\kappa_H} &= \frac{\partial \mathcal{R}_0}{\partial \kappa_H} \cdot \frac{\kappa_H}{\mathcal{R}_0}, & \Phi_{\mathcal{R}_0}^{\kappa_M} &= \frac{\partial \mathcal{R}_0}{\partial \kappa_M} \cdot \frac{\kappa_M}{\mathcal{R}_0}, \\ \Phi_{\mathcal{R}_0}^\alpha &= \frac{\partial \mathcal{R}_0}{\partial \alpha} \cdot \frac{\alpha}{\mathcal{R}_0}, & \Phi_{\mathcal{R}_0}^\eta &= \frac{\partial \mathcal{R}_0}{\partial \eta} \cdot \frac{\eta}{\mathcal{R}_0}. \end{aligned}$$

This analysis provides a systematic framework for quantifying the effects of parameter variations on the \mathcal{R}_0 and other critical outcomes. Using the aforementioned expression equation (19), we calculate the sensitivity index of \mathcal{R}_0 in relation to temperature and rainfall based on the parameter values presented in Table 2. The results are visually represented in Figures (9, 10). Parameters exhibiting positive sensitivity indices imply that reducing their values could effectively contribute to reducing malaria transmission. Conversely, increasing the values of parameters with negative index may also help mitigate the spread of the disease.

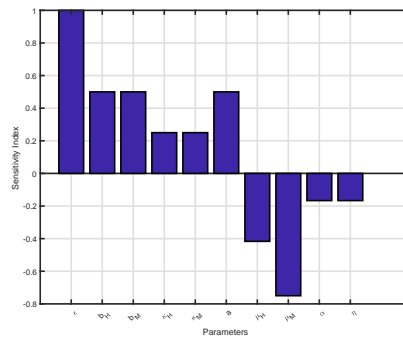


Figure 8: Sensitivity indices of parameters related \mathcal{R}_0 .

Analysis of these figures demonstrates that indicate that the sensitivity index of \mathcal{R}_0 in relation to rainfall is not significantly influenced by temperature and tends to decrease as rainfall increases. In contrast, the sensitivity index of \mathcal{R}_0 concerning temperature shows that as temperatures rise, the index shifts from positive to negative once it exceeds 28.8°C . This finding suggests that moderate increases in temperature can enhance malaria transmission, while higher temperatures tend to suppress it. Additionally, the sensitivity index of \mathcal{R}_0 concerning temperature exhibits only slight changes when rainfall levels vary.

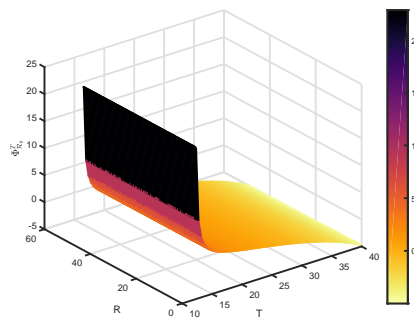


Figure 9: Sensitivity index of the basic reproduction number (\mathcal{R}_0) in relation to temperature (T). The graph shows the impact of temperature fluctuations on the disease's potential for transmission.

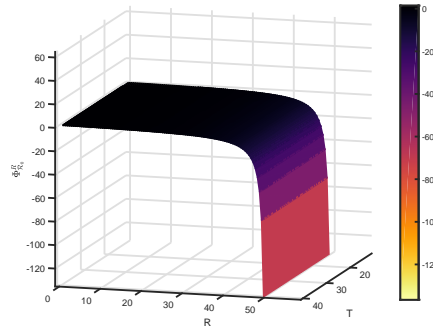


Figure 10: The sensitivity index of the basic reproduction number (\mathcal{R}_0) concerning rainfall (R) is depicted in the plot. It highlights the impact of varying rainfall patterns on disease transmission dynamics.

4 The Global Stability of Disease-Free Equilibrium

We examine the global stability of the DFE as follows.

Lemma 2. From (11), the system can be expressed as:

$$\begin{cases} \frac{dA_d}{dt} = f(A_d, A_s), \\ \frac{dA_s}{dt} = g(A_d, A_s), \end{cases} \quad (20)$$

where $A_d = (E_H, I_H, R_H, E_M, I_M)^T$ represents the infectious compartments including the recovering population, and $A_s = (S_H, S_M)^T$ corresponds to the disease-free compartments. Let $A_0^* = (A_s^*, 0)$ denotes the DFE of the system. Assume the following conditions:

- C_1 : $\frac{dA_s}{dt} = f(A_s, 0)$, and A_s^* is globally asymptotically stable.
- C_2 : $\frac{dA_d}{dt} = g(A_s, A_d) = A_d - \hat{g}(A_s, A_d)$, where $\hat{g}(A_s, A_d) \geq 0$ for $(A_s, A_d) \in \Gamma$.

The Jacobian matrix $A = \frac{\partial g}{\partial A_d}(A_s^*, 0)$ is an M-matrix (Metzler matrix with non-negative diagonal elements). In the region Γ , the model is considered biologically plausible.

Theorem 2. The disease-free equilibrium point (E_0) of the system (4) is globally asymptotically stable if $\mathcal{R}_0 < 1$.

Proof. Consider the model system (4), and let

$$A_s = (S_H, S_M)^T \text{ and } A_d = (E_H, I_H, R_H, E_M, I_M)^T.$$

Then

$$\frac{dA_s}{dt} = f(A_s^*, 0) = \begin{bmatrix} \theta - \mu_H S_H \\ 0 \\ 0 \\ \eta - \mu_M S_M \\ 0 \end{bmatrix}. \quad (21)$$

As a result, condition C_1 is clearly met. Next, we verify condition C_2

$$AA_d = \begin{bmatrix} -(\kappa_H + \mu_H) & 0 & 0 & 0 & 0 \\ \kappa_H & -(\mu_H + \alpha + \eta) & 0 & 0 & 0 \\ 0 & \alpha & -(\gamma + \mu_H) & 0 & 0 \\ 0 & 0 & 0 & -(\kappa_M + \mu_M) & 0 \\ 0 & 0 & 0 & \kappa_M & -\mu_M \end{bmatrix} \begin{bmatrix} E_H \\ I_H \\ R_H \\ E_M \\ I_M \end{bmatrix}, \quad (22)$$

It is evidently an M-matrix, characterized by positive off-diagonal elements. Now,

$$g(A_s, A_d) = \begin{bmatrix} \Lambda_H S_H - (\kappa_H + \mu_H) E_H \\ \kappa_H E_H - (\mu_H + \alpha + \eta) I_H \\ \alpha I_H - (\gamma + \mu_H) R_H \\ \Lambda_M S_M - (\kappa_M + \mu_M) E_M \\ \kappa_M E_M - \mu_M I_M \end{bmatrix}. \quad (23)$$

From Lemma 2, we have

$$\hat{g}(A_s, A_d) = AA_d - g(A_s, A_d),$$

yields

$$\hat{g}(A_s, A_d) = \begin{bmatrix} -(\kappa_H + \mu_H) E_H \\ \kappa_H E_H - (\mu_H + \alpha + \eta) I_H \\ \alpha I_H - (\gamma + \mu_H) R_H \\ -(\kappa_M + \mu_M) E_M \\ \kappa_M E_M - \mu_M I_M \end{bmatrix} - \begin{bmatrix} \Lambda_H S_H - (\kappa_H + \mu_H) E_H \\ \kappa_H E_H - (\mu_H + \alpha + \eta) I_H \\ \alpha I_H - (\gamma + \mu_H) R_H \\ \Lambda_M S_M - (\kappa_M + \mu_M) E_M \\ \kappa_M E_M - \mu_M I_M \end{bmatrix}. \quad (24)$$

Simplifying

$$\hat{g}(A_s, A_d) = \begin{bmatrix} \Lambda_H S_H \\ 0 \\ 0 \\ \Lambda_M S_M \\ 0 \end{bmatrix}. \quad (25)$$

Since $0 \leq S_H \leq S_M \leq N$, we have $\hat{g}(A_s, A_d) \geq 0$. As a result, condition C_2 is met. Hence, the DFE of the model is globally asymptotically stable whenever $\mathcal{R}_0 < 1$. \square

5 Numerical Simulations

This section explores the complex interplay between climate change and malaria dynamics, highlighting the importance of a robust mathematical model in guiding effective control measures and policy decisions to mitigate the global impact of malaria. To investigate the impact of climatic variables on malaria prevalence within a community, we utilize MATLAB solver *ode45* to simulate the equations in our system. Matlab offers a variety of built-in solvers for differential equations, which are particularly beneficial for initial value ordinary differential equation problems. Among these, *ode45* stands

out as a sophisticated and widely adopted function renowned for delivering highly accurate solutions. This solver simultaneously employs fourth- and fifth-order Runge-Kutta methods, specifically using the Dormand-Prince pair. As a one-step solver, *ode45* is often the preferred choice for many problems, efficiently managing non-stiff equations. By default, it utilizes extended step sizes and calculates solution values at four equally spaced points within each natural step interval.

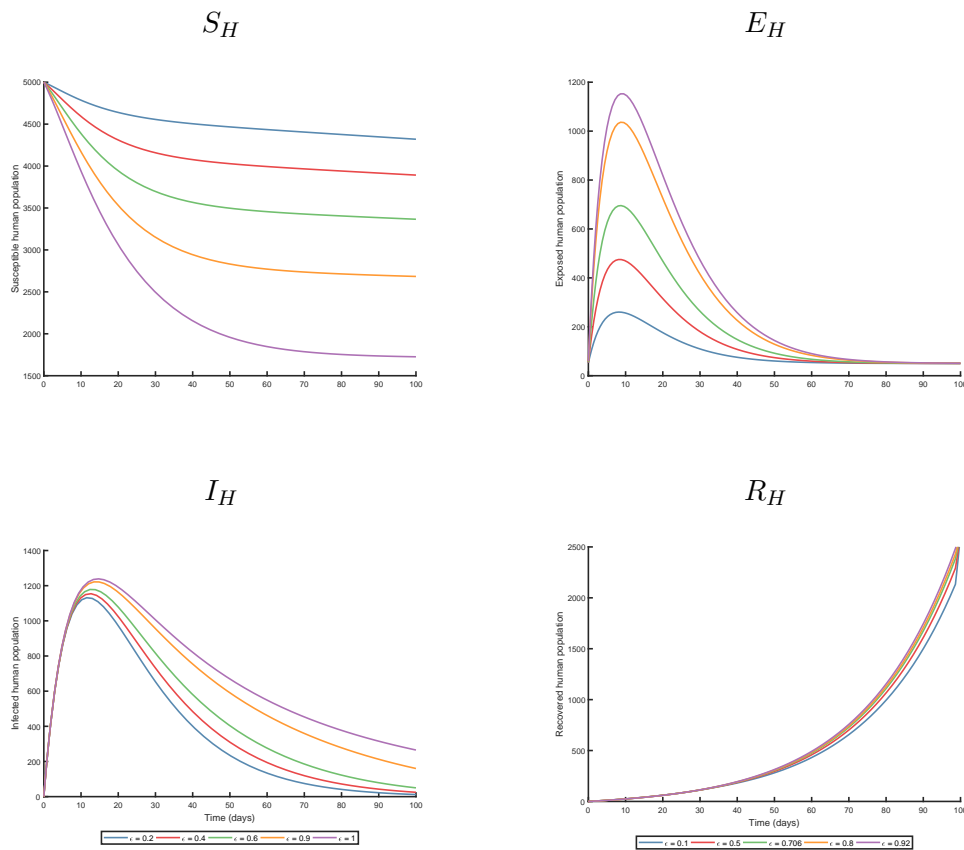


Figure 11: Malaria dynamics in the human population in the system (4) by varying the mosquito bite rate ϵ due to climate dependence.



In our research approach, we concurrently adjust multiple climate variables to evaluate the parameter of interest (see Figures 3 and 4). In Figure 2, ϵ_0 reflects the baseline biting rate, while β is a parameter that

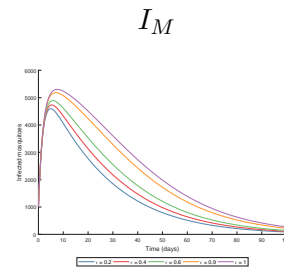


Figure 12: Malaria dynamics in the mosquito population in the system (4) through an examination of varying ϵ due to climate dependence.

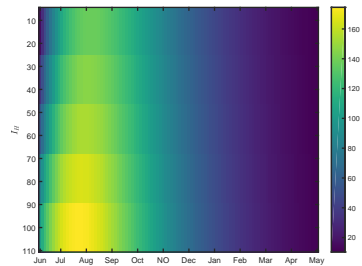


Figure 13: Profile of infectious human population I_H .

modulates the saturation effect, acknowledging the potential decrease in mosquito breeding habitats that can occur with excessive rainfall. The accompanying color map effectively visualizes the fluctuations in biting rate relative to varying temperature and rainfall scenarios. We also designate a specific climate variable as a constant to gauge the impact of each parameter on the outcomes while averaging the effects of the remaining variables (refer to Figure 5). This experimental framework is designed to identify the parameters of greatest significance. By assuming a monotonic relationship between each parameter and the number of preventions achieved, we can investigate these relationships through partial rank correlations between each parameter and the number of infections averted. This experimental analysis underscores the varying influences of different parameters on the efficacy of vector control strategies, highlighting the critical roles of temperature and relative humidity in malaria transmission dynamics. We observed that when the extrinsic incubation period (the time that a mosquito needs to become infectious after feeding on an infected host) is shorter than the average lifespan of a mosquito, control efforts should prioritize reducing the frequency of mosquito bites.

Our analysis spans a time frame from $t = 0$ to $t = 100$, revealing trends in the patterns illustrated in Figures 11 and 12 for human and mosquito populations, respectively. The detailed parameters employed in these simulations are presented in Table 2. Through the analysis of simulations with diverse parameter values, we have gleaned significant insights into the behavioral patterns and transmission dynamics of malaria in Sudan, particularly in light of environmental factors. This exploration highlights the complex interplay between various ecological elements and malaria epidemiology, offering a deeper

understanding of the disease's spread and potential control measures. Data suggests that rainfall exerts little influence on the survival rates of adult mosquitoes, whereas temperature significantly impacts their longevity. These simulations corroborate our theoretical findings, emphasizing the relevance of our proposed mathematical methodologies in advancing the understanding of malaria transmission and informing effective control strategies. Our comprehensive numerical simulations have elucidated the theoretical concepts, establishing a solid foundation for future investigations in this essential domain of public health.

A qualitative examination of the malaria transmission model provided insights into the stability of the disease-free equilibrium at both local and global scales, while also allowing for a detailed assessment of equilibrium solutions through the computation of the basic reproduction number. Figure 13 illustrate the effects of environmental factors, i.e., temperature and rainfall, on the dynamics of mosquito-borne disease, with a particular focus on the infected human population over time. The study particularly emphasizes the impact of rainfall and temperature variations on human transmission dynamics. The findings reveal that the highest abundance of mosquitoes occurs within a temperature range of 25°C and 30°C and rainfall measurements between 120 and 150mm. Through simulations across different parameter ranges, we assessed the efficacy of various intervention strategies aimed at reducing the malaria burden (see Figures 11 and 12).

The basic reproductive number on Figure 6 provides a basis for further refinement and prediction of the effect of climate variability on the intensity of malaria transmission. We can see in Figure 8 the impact for each parameter (positive sign and negative sign as mentioned above) in \mathcal{R}_0 . Figures 9 and 10 show the sensitivity index \mathcal{R}_0 concerning T and R . We observe that when the rainfall averages 50 mm, temperatures below 35.7°C lead to a proportional decrease in the disease transmission, with the disease course declining as temperatures increase, reaching zero when the temperature reaches 32.6°C. We also note that when rainfall is around 90 or 110 mm, temperatures below 28.8°C have a more positive effect. Furthermore, as the temperature increases, the relative increase decreases to zero when the temperature reaches 28.8°C.

6 Concluding Remarks and Future Research Directions

This study has explored the critical link between climate change and malaria transmission in Sudan. The findings indicates a concerning rise in malaria cases in recent years, with Sudan experiencing the heaviest burden among affected nations. Through the use of a deterministic mathematical model, we have rigorously analyzed the complex interactions between climatic variables—particularly temperature and rainfall—and the dynamics of malaria transmission. The results underscore the significant influence of these environmental factors on the growth and distribution of malaria vectors, highlighting the necessity for immediate actions to mitigate the adverse effects of climate change. By assessing the stability of various equilibrium solutions under different scenarios, we have gained valuable insights into the resilience of malaria transmission patterns amid evolving climatic conditions. The calculation of the basic reproduction number R_0 further illuminated how sensitive malaria transmission is to fluctuations in temperature and rainfall. Simulation results, based on calibrated parameters, confirm the increasing role of climate factors in shaping the epidemiological landscape of malaria. These findings emphasize the

importance of integrated strategies that combine climate change adaptation with robust malaria control measures. Addressing the primary drivers of transmission—especially climate variability—will facilitate the development of more effective interventions to reduce disease burden. Looking forward, continued research and collaboration are essential for safeguarding public health and strengthening resilience against the shifting malaria landscape in the context of climate change.

Future Research Scope

We intend to incorporate stochastic approaches alongside deterministic models to better capture the probabilistic nature of transmission determinants, which are not always predictable through deterministic frameworks. Depending on the data availability and research objectives, spatial modeling of disease spread—either continuous or discrete—will be explored. This dual approach allows a deeper understanding of the complex dynamics governing transmission and their impact on disease spread. Additionally, spatial modeling techniques, whether continuous or discrete, can be augmented with artificial neural networks, (e.g., see more in [14]) to analyze and predict disease spread more effectively, addressing the multifaceted nature of transmission processes.

Declarations

Availability of Supporting Data

All data generated or analyzed during this study are included in this published paper.

Funding

The research of K.C.P. contained in this paper was supported by the South African National Research Foundation.

Competing Interests

The authors declare that they have no competing interests relevant to the content of this paper.

Authors' Contributions

The research theme presented was conceived by all authors. The mathematical model was refined by G.A.M.O.F, K.C.P, A.M. wrote the preliminary draft of the manuscript and further improved it under the supervision of G.A.M.O.F, K.C.P, A.M. conducted numerical simulations. A.M. and K.C.P. assisted with analytical details and validation of simulations while supervising the main findings of this study. All authors engaged in discussions regarding the results and contributed equally to the final manuscript.

References

- [1] Abdelrazecy, A., Okuneye, K., Gumel, A.B. (2018). “Mathematical analysis of a weather-driven model for the population ecology of mosquitoes”, *Mathematical Biosciences & Engineering*, 15(1), 57-93, [doi:10.3934/mbe.2018003](https://doi.org/10.3934/mbe.2018003).
- [2] Abdu, Z., Mohammed, Z., Bashier, I., Eriksson, B. (2004). “The impact of user fee exemption on service utilization and treatment seeking behaviour: The case of malaria in Sudan”, *The International Journal of Health Planning and Management*, 19(1), 95-106, [doi:10.1002/hpm.777](https://doi.org/10.1002/hpm.777).
- [3] Adam, I., Ibrahim, Y., Elhardello, O. (2018). “Prevalence, types, and determinants of anemia among pregnant women in Sudan: A systematic review and meta-analysis”, *BMC Hematology*, 18(1), 1-8, [doi:10.1186/s12878-018-0124-1](https://doi.org/10.1186/s12878-018-0124-1).
- [4] Akbari, R., Leader, N., Mohammad, S. (2024). “Dynamical behaviour of fractional order SEIR mathematical model for infectious disease transmission”, *Control and Optimization in Applied Mathematics*, 9(1), 35-48, [doi:10.30473/coam.2023.64849.1210](https://doi.org/10.30473/coam.2023.64849.1210).
- [5] Baker, R.E., Mahmud, A.S., Miller, I.F., Rajeev, M., Rasambainarivo, F., Rice, B.L., Takahashi, S., Tatem, A.J., Wagner, C.E., Wang, L.F., Wesolowski, A. (2022). “Infectious disease in an era of global change”, *Nature Reviews Microbiology*, 20(4), 193-205, [doi:10.1038/s41579-021-00639-z](https://doi.org/10.1038/s41579-021-00639-z).
- [6] Beck-Johnson, L.M., Nelson, W.A., Krijn, P.P., Read, A.F., Thomas, M.B., Bjørnstad, O.N. (2013). “The effect of temperature on Anopheles mosquito population dynamics and the potential for malaria transmission”, *PLOS One*, 8(11), 79276, [doi:10.1371/journal.pone.0079276](https://doi.org/10.1371/journal.pone.0079276).
- [7] Birkhoff, G., Carlo-Rota, G. (1989). “Ordinary differential equations”, John Wiley & Sons Inc John Wiley and Sons Inc., New York, USA.
- [8] Blanford, J.I., Blanford, S., Crane, R.G., Mann, M.E., Paaijmans, K.P., Schreiber, K.V., Thomas, M.B. (2013). “Implications of temperature variation for malaria parasite development across Africa”, *Scientific Reports*, 3(1) 1-11, [doi:10.1038/srep01300](https://doi.org/10.1038/srep01300).
- [9] Chitnis, N., Smith, T., Steketee, R. (2008). “A mathematical model for the dynamics of malaria in mosquitoes feeding on a heterogeneous host population”, *Journal of Biological Dynamics*, 2(3), 259-285, [doi:10.1080/17513750701769857](https://doi.org/10.1080/17513750701769857).
- [10] Cobremesk, A.A., Krogstad, H.E. (2015). “Mathematical modeling of endemic transmission”, *American Journal of Applied Mathematics*, 3(2), 36-46, [doi:10.11648/j.ajam.20150302.12](https://doi.org/10.11648/j.ajam.20150302.12).
- [11] Coetzee, M., Horne, D.W.K., Brooke, B.D., Hunt, R.H. (1999). “DDT, dieldrin and pyrethroid insecticide resistance in African malaria vector mosquitoes: An historical review and implications for future malaria control in southern Africa”, *South African Journal of Science*, 95(5), 215-218.
- [12] Craig, M.H., Sauer, D.L., Snow, B. (1999). “A climate-based distribution model of malaria transmission in Sub-Saharan Africa”, *Parasitology Today*, 15(3), 105-111, [doi:10.1016/S0169-4758\(99\)01396-4](https://doi.org/10.1016/S0169-4758(99)01396-4).

- [13] Dafallah, E.S., El-Agib, F.H., Bushra, G.O. (2003). "Maternal mortality in a teaching hospital in Sudan", *Saudi Medical Journal*, 24(4), 369-372.
- [14] Dastjerdi, R.H., Ahmadi, G., Dadkhah, M., Ayatillah, Y. (2023). "Optimal control of infectious disease using the artificial neural networks", *Control and Optimization in Applied Mathematics*, 8(2), 17-32, [doi:10.30473/coam.2023.64776.1208](https://doi.org/10.30473/coam.2023.64776.1208).
- [15] Driessche, P.V.d., Watmough, J. (2002). "Reproduction numbers and sub-threshold endemic equilibria for compartmental models of disease transmission", *Mathematical Biosciences*, 180(1-2), 29-48, [doi:10.1016/S0025-5564\(02\)00108-6](https://doi.org/10.1016/S0025-5564(02)00108-6).
- [16] Gashaw, K.W., Kassa, S.M., Ouifki, R. (2019). "Climate-dependent malaria disease transmission model and its analysis", *International Journal of Biomathematics*, 12(8), 1950087, [doi:10.1142/S1793524519500876](https://doi.org/10.1142/S1793524519500876).
- [17] Hoshen, M.B., Morse, A.P. (2004). "A weather-driven model of malaria transmission", *Malaria Journal*, 3(1), 1-14, [doi:10.1186/1475-2875-3-32](https://doi.org/10.1186/1475-2875-3-32).
- [18] Joe, K., Ogana, W., Nyandwi, S., Kwizera, J.D.D., Niyukuri, D. (2024). "A mathematical model exploring the impact of climatic factors on malaria transmission dynamics in Burundi", *Journal of Applied Mathematics and Physics*, 12(11), 3728-3757, [doi:10.4236/jamp.2024.1211224](https://doi.org/10.4236/jamp.2024.1211224).
- [19] Kuehn, A., Pradel, G. (2010). "The coming-out of malaria gametocytes", *Journal of Biomedicine and Biotechnology*, 2010(1), [doi:10.1155/2010/976827](https://doi.org/10.1155/2010/976827).
- [20] Lindsay, S.W., Birley, M.H. (1996). "Climate change and malaria transmission", *Annals of Tropical Medicine & Parasitology*, 90(5), 573-588, [doi:10.1080/00034983.1996.11813087](https://doi.org/10.1080/00034983.1996.11813087).
- [21] Martens, W.J., Louis, W.N., Rotmans, J., Jetten, T.H., McMichael, J.A. (1995). "Potential impact of global climate change on malaria risk", *Environmental Health Perspectives*, 103(5), 458-464, [doi:10.1289/ehp.95103458](https://doi.org/10.1289/ehp.95103458).
- [22] Mordecai, E.M., Ryan, S.J., Caldwell, J.M., Shah, M.M., LaBeaud, A.D. (2020). "Climate change could shift disease burden from malaria to arboviruses in Africa", *The Lancet Planetary Health*, 4(9), [doi:10.1016/S2542-5196\(20\)30178-9](https://doi.org/10.1016/S2542-5196(20)30178-9).
- [23] Mukhtar, A.Y.A., Munyakazi, J.B. Ouifki, R. (2019). "Assessing the role of climate factors on malaria transmission dynamics in South Sudan", *Mathematical Biosciences*, 310, 13-23, [doi:10.1016/j.mbs.2019.01.002](https://doi.org/10.1016/j.mbs.2019.01.002).
- [24] National malaria control programme (NMCP), Sudan (2024), <https://mesamalaria.org/institution/national-malaria-control-programme-nmcp-sudan/>.
- [25] Ngarakana-Gwasira, E.T., Bhunu, C.P., Masocha, M., Mashonjowa, E. (2016). "Assessing the role of climate change in malaria transmission in Africa", *Malaria Research and Treatment*, 2016(1), [doi:10.1155/2016/7104291](https://doi.org/10.1155/2016/7104291).
- [26] Osman, A.A., Osman, Y.E., Ibrahim, Y., Mussa, A., Mohamed, Z., Suppain, R., Hajissa, K. (2022). "Prevalence of malaria among clinically suspected patients and pregnant women in Sudan: A systematic review and meta-analysis", *SN Comprehensive Clinical Medicine*, 4(1), 1-12, [doi:10.1007/s42399-022-01160-x](https://doi.org/10.1007/s42399-022-01160-x).

- [27] Paaijmans, K.P., Cator, L.J., Thomas, M.B. (2013). “Temperature-dependent pre-bloodmeal period and temperature-driven asynchrony between parasite development and mosquito biting rate reduce malaria transmission intensity”, *PLOS One*, 8(1), e55777, [doi:10.1371/journal.pone.0055777](https://doi.org/10.1371/journal.pone.0055777).
- [28] Paaijmans, K.P., Blanford, S., Bell, A.S., Blanford, J.I., Read, A.F., Thomas, M.B. (2010). “Influence of climate on malaria transmission depends on daily temperature variation”, *Proceedings of the National Academy of Sciences*, 107(34), 15135-15139, [doi:10.1073/pnas.1006422107](https://doi.org/10.1073/pnas.1006422107).
- [29] Tran, A., L’Ambert, G., Lacour, G., It, R.B., Demarchi, M., Cros, M., Cailly, P., AubryKientz, M., Balenghien, T., Ezanno, P. (2013). “A rainfall-and temperature-driven abundance model for *Aedes albopictus* populations”, *International Journal of Environmental Research and Public Health*, 10(5), 1698-1719, [doi:10.3390/ijerph10051698](https://doi.org/10.3390/ijerph10051698).
- [30] World health organization (WHO) and global malaria programme (2022).
- [31] Yang, H.M. (2000). “Malaria transmission model for different levels of acquired immunity and temperature dependent parameters vector”, *Revista de Saude Publica*, 34, 223-231, [doi:10.1590/S0034-89102000000300008](https://doi.org/10.1590/S0034-89102000000300008).